Load-resistance analysis: An alternative approach to tsunami damage assessment applied to the 2011 Great East Japan tsunami

Anawat Suppasri[1], Kwanchai Pakoksung[1], Ingrid Charvet[2], Constance Ting Chua[3], Noriyuki Takahashi[4], Teraphan Ornthammarath[5], Panon Latcharote[6], Natt Leelawat[7] and Fumihiko Imamura[1]

[1]International Research Institute of Disaster Science, Tohoku University
(468-1 Aramaki-aza Aoba, Aoba-ku, Sendai 980-0845, Japan)
[2]Department of Statistical Science, University College London, United Kingdom
(Gower Street, London, WC1E 6BT)
[3]Asian School of the Environment, Nanyang Technological University
(N2-01C-39, 50 Nanyang Avenue, Singapore 639798)
[4]Department of Architecture and Building Science, School of Engineering, Tohoku University
(6-6-11-1223 Aramaki-aza Aoba, Aoba-ku, Sendai 980-8579, Japan)
[5]Department of Civil and Environmental Engineering, Faculty of Engineering, Mahidol University
(25/25 Puttamonthon, Nakorn Pathom, 73170, Thailand)
[6]Faculty of Science and Technology, Thammasat University
(99 Moo 18, Phaholyothin Road, Tambon Klong Nung, Amphoe Klong Luang, Pathum Thani 12120, Thailand)
[7]Disaster and Risk Management Information Systems Research Group, Department of Industrial Engineering, Faculty of Engineering, Chulalongkorn University
(Phayathai Road, Pathumwan, Bangkok 10330 Thailand)

Abstract

Tsunami fragility functions describe the probability of structural damage to tsunami flow characteristics. Fragility functions developed from past tsunami events (e.g. 2004 Indian Ocean tsunami) are often applied directly, without modifications, to other areas at risk of tsunami for the purpose of damage and loss estimations. Consequentially, estimates carry uncertainty due to disparities in construction standards and coastal morphology between the specific region for which the fragility functions were originally derived and the region where they were being used. The main objective of this study is to provide an alternative approach to assessing tsunami damage, especially for buildings in regions where previously developed fragility functions do not exist. A damage assessment model is proposed in this study, where load-resistance analysis is performed for each building by evaluating hydrodynamic forces, buoyancies and debris impacts and comparing them to the resistance forces of each building. Numerical simulation was performed in this study to reproduce the 2011 Great East Japan tsunami in Ishinomaki city, which is chosen as a study site. Flow depths and velocities were calculated for approximately 20, 000 wooden buildings in Ishinomaki city. Similarly, resistance forces (lateral and vertical) are estimated for each of these buildings. The buildings are then evaluated for its potential to collapse. Results from this study reflect a higher accuracy in predicting building collapse when using the proposed load-resistance analysis as compared to previously developed fragility functions in the same study area. Damage is also observed to have likely occurred before flow depth and velocity reach maximum values. With the above considerations, the proposed damage model might well be an alternative for building damage assessments in areas which have yet to be affected by modern tsunami events.

Higher resolution figures are attached in the supplementary file.

1. Introduction

The 2011 Great East Japan earthquake generated a large tsunami which damaged and destroyed more than 250, 000 buildings (MLIT, 2012). Building damage characteristics from the 2011 event have since been well-studied and in most cases, used to develop tsunami damage fragility functions (Suppasri et al., 2015). Tsunami damage fragility functions describe the probability of structural damage to tsunami flow characteristics, i.e. flow depth, flow velocity and hydrodynamic force. Fragility functions have been developed from past events (e.g. 2004 Indian Ocean, 2010 Chile and 2011 Great East Japan tsunamis) and are often applied directly, without modifications, to other areas facing tsunami risk for damage and loss assessments (Suppasri et al., 2016). The resulting damage estimates carry uncertainty related to differences in construction standards and coastal morphology between the specific region for which the fragility functions were originally derived and the region where they are being used.

Tsunami fragility functions are modelled using tsunami flow characteristics and building damage information. In general, the methods for deriving tsunami fragility functions can be classified into four categories.

(1) Empirical methods based on statistical analysis of observed post tsunami damage data (e.g., Peiris, 2006, Reese et al., 2007, Dias et al. 2009, Valencia et al., 2011, Suppasri et al. 2015 and Triantafyllou et al., 2018). In a field survey, maximum flow depth measured from tsunami water traces are typically used as explanatory variables of damage. Building damage data is obtained from on-site observations.

(2) Hybrid techniques that combine tsunami hazard mapping (numerical simulation of tsunami inundation such as maximum flow depth, maximum flow velocity and maximum hydrodynamic force) with interpreted building damage data from remote sensing and (e.g., Koshimura et al. 2009, Omira et al., 2010 and Suppasri et al. 2011) or other damage data set such as damaged marine vessels (Suppasri et al., 2014), damaged bridges (Shoji and Nakamura, 2017) as well as aquaculture rafts and eelgrass (Suppasri et al., 2018).

(3) Heuristic fragility functions based on expert opinion such as HAZUS (FEMA 2013) and Papathoma Tsunami Vulnerability Assessment (PTVA) (Dall'Osso et al., 2016).

(4) Analytical fragility functions based on structural modelling and response simulations (e.g. Macabuag et al. 2014, Nanayakkara and Dias 2016 and Attary et al. 2017).

Recent studies have shown tsunami hydrodynamic force to be an important explanatory parameter (Macabuag et al., 2016), flow velocity at time of occurrence (Song et al., 2018) and floating debris (Macabuag et al., 2018) are all factors when assessing building damage. In order to obtain fragility functions for areas where tsunami data is not yet available, it is necessary to model the deterministic processes relating tsunami characteristics to the capacity of the structure to resist resulting loads. This allows for the structural characteristics information specific to the buildings of a region to be taken into account, as well as bypassing the use of potentially biased observed values for the explanatory variables. This study proposes an alternative approach to tsunami damage assessment by not rely on pre-developed fragility functions but by investigating interactions between tsunami loading and the structural resistance of a system (in this case the resistance of a building) through an analytical model to infer tsunami damage. The objective is to provide an alternative approach to assessing tsunami damage especially for buildings in areas where previously developed fragility functions do not exist. As part of this study, tsunami characteristics at the time of damage occurrence will be investigated and used in the proposed model to provide a complementary insight into the relationship between structural damage and tsunami flow characteristics.

The analytical model is defined following an overview of tsunami flow characteristics and their effects on buildings. Next, the study site and building damage data set used to demonstrate the application of the model are presented. Two major components of the model are then discussed: tsunami numerical simulation and the estimation of resisting forces. Model results are compared to other building damage assessment estimates and observations in order to examine their applicability in building damage estimation. In addition, because structural damage is usually presented in a qualitative manner, most tsunami damage assessments may not be readily usable by private or governmental organisations. Therefore, a financial metric converting existing structural damage levels into financial cost ratios is proposed.

2. Alternative approach to tsunami damage assessment

Damage by tsunamis to infrastructure are caused by many factors such as tsunami forces, impact of waterborne debris, building characteristics and scouring of foundations (Kelman and Spence, 2004). Forces generated by a tsunami can be estimated by classifying them according to their flow conditions and characteristics. Hydrodynamic force is generated by the pressure from flowing waters around the structure, and is influenced by flow velocity, depth and density of the water as well as the geometry and angle at which the tsunami hits the structure (Nadal et al., 2010). When hydrodynamic force is used in tsunami science, it usually refers to the drag force which is directly proportional to the square of flow velocity. Debris impact force is driven by tsunami flow. Tsunami-borne debris, while not a direct action of tsunami flow, can cause substantial damage to buildings. It can result in the reduction of load-bearing capacity in a building, and therefore the reduction in structural resistance to lateral loads and buoyancy forces (Nadal et al., 2010).

The approach taken in this study is an adaptation from Latcharote et al (2017) where they analysed and compared the overturning mechanism with resisting moment for six overturned reinforced concrete buildings in Onagawa town. Similarly, the proposed damage model performs load-resistance analysis for each building by evaluating hydrodynamic forces, buoyancy forces and debris impacts and comparing them to the resistance of each building. There are two general types of resistance that a building provides. First, it provides lateral resistance which is designed to counter loads that are perpendicular to and imposed on walls. Second, the weight of the buildings acts as downward-acting (vertical) resistance against buoyancy forces or upward-acting loads from wind and seismic activities. The resistance force from pile foundation was also one of the components examined in Latcharote et al. (2017). However, because wooden buildings were used for this study, the resistance force from pile foundation was not considered.

Global stability failure in a building can be a result of either sliding or overturning as a solitary body, often with minimal damage to structural/non-structural components (Yeh et al, 2014). Overturning refers to the rotation of a building around its foundation where it has failed. Sliding, on the other hand, is the horizontal translation of a building from its original position (Yeh et al, 2014). The two mechanisms are modelled separately in this study to determine the predominant mechanism for building collapse. Differences in the forces and resistance involved in these mechanisms were considered when performing load-resistance analysis:

(1) Sliding/Non-submerged at the point of impact (**Fig. 1 (a)**): Only horizontal hydrodynamic force, debris impact and lateral resistance of the building were considered in this case. A building collapses if the compounded hydrodynamic and debris impact forces are greater than the lateral resistance of the building.
(2) Overturning/Submerged (**Fig. 1 – (b)**): A building collapses when the overturning moment from hydrodynamic and buoyancy forces is greater than the resisting moment from the building weight. Under such circumstances, the building can either be fully submerged as illustrated in

Fig. 1 (**b**) or surrounded by water with no water inside. In the former case, when the building is completely inundated, forces from the exterior of the building are cancelled out. The latter is the worst-case scenario and is assumed for subsequent analyses of overturning mechanisms in this study.

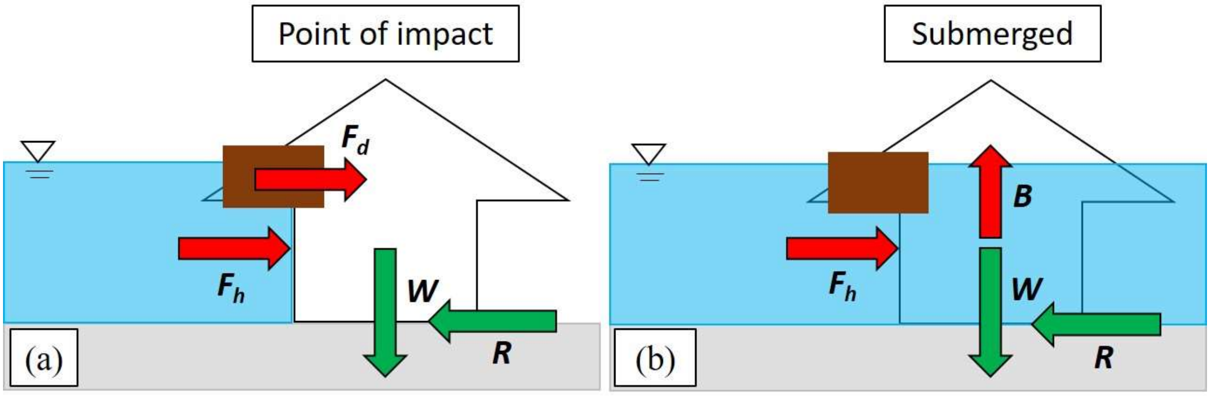

Fig.1 Two failure mechanisms are considered in this study: (a) Sliding and (b) overturning. The forces denoted are as follows, F_h = hydrodynamic force, F_d = debris impact force, R = lateral resistance, W = building weight and B = buoyancy force.

2.1 Selection of study site

There were many possible areas for studying building damage from the 2011 Great East Japan tsunami event. A suitable study site needs to be highly representative of the processes being modelled, without excessive contributions of un-modelled effects. In addition, a previously investigated area would allow for a fair assessment of the analytical model's results. Ishinomaki City, Miyagi Prefecture was therefore selected as the area displayed the following characteristics:

1. Less impact from wave amplification: Ishinomaki City is located on a plain coast which reduces the effects of wave amplification unlike coastal towns located along the Sanriku Ria Coast
2. Less impact from floating debris: The populated areas of Ishinomaki are far from fishing ports and storage facilities, many of which were damaged by the tsunami and generated floating debris, which can magnify building damage. Floating debris from broken pine trees can also be excluded from consideration as the coastal pine forest along the city survived.
3. Less impact from wave directions: The effects from varying wave directions are minor as most of the buildings were lined facing the shoreline and the direction of wave attack was perpendicular to the front of the buildings.
4. Largest sample size: The number of buildings affected by the 2011 event was largest in Ishinomaki City amongst cities along the plain coast.
5. Previously developed fragility functions: Fragility functions have been previously developed for the populated areas of Ishinomaki City (Charvet et al., 2014). A new study from Hasegawa et al., (2018) provides an excellent opportunity to compare the proposed method in this study with the established model.

2.2 Building damage data

Detailed building damage data from field observations was obtained from the Ministry of Land, Infrastructure and Transportation and Tourism (MLIT) (MLIT, 2012) (**Fig. 2**) to test the applicability of the proposed building damage model. The data consists of building size (length and width), number of stories, construction material and interpolated measured maximum flow depth of each building. Each building was also classified according to their observed damage. There are a total of six damage levels in the classification scheme by MLIT. Low damage levels (i.e. levels 1 – 4) are easily misclassified in damage assessments due to overlapping descriptions in the classification scheme (Leelawat et al., 2014), whereas damage levels 5 and 6 are straightforward in their definitions (**Fig. 3**). "Washed away" and "destroyed" (levels 5 and 6) refer to structures which are irreparable. In this study, the two levels "washed away" and "destroyed" are considered since sliding and overturning mechanisms fall into the aforementioned categories. As opposed to lower damage levels, these damage modes are driven by the structural properties of these buildings, thus only buildings damaged at these levels were used for this study. The building type considered in this pioneer study is only wooden residential houses due to their large sample size in this area.

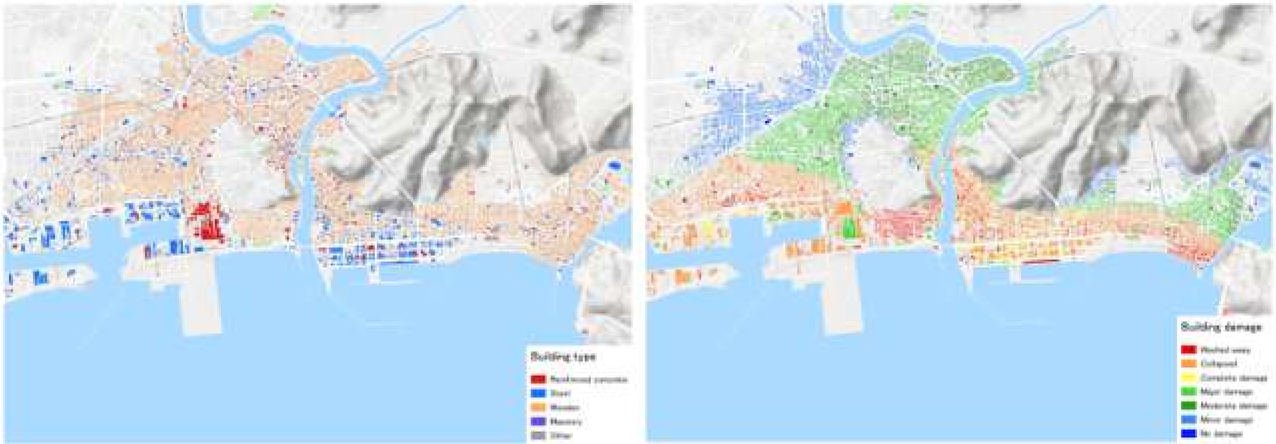

Fig.2 (Left) Distributions of building types and (Right) building damage levels.

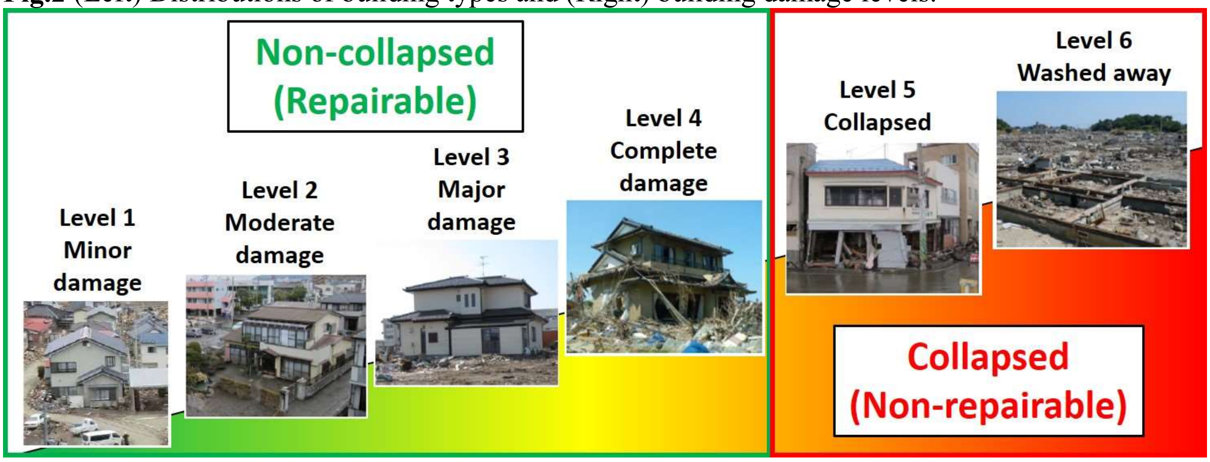

Fig. 3 Building damage levels and collapsed condition considered in this study (courtesy of MLIT, 2012).

2.3 Numerical simulation of the 2011 tsunami and damage inducing forces

Tsunami flow characteristics (flow depth, velocity and hydrodynamic force) at the point of damage occurrence were estimated in a time series analysis of the 2011 Great East Japan tsunami, which was reproduced by numerical simulation. The numerical model computed tsunami propagation and run-up by using a set of nonlinear shallow water equations which were solved by staggered leap-frog finite difference scheme, and bottom frictional values were written using Manning's formula (Suppasri et al., 2011, Charvet et al., 2015 and Macabaug et al., 2016). The model set-up includes the preparation of bathymetry and topography data – a nested grid system consisting of six computational domains – 1215 m (Region 1), 405 m (Region 2), 135 m (Region3), 45 m (Region 4), 15 m (Region 5) and 5 m (Region 6) was used for the study area (**Fig. 4**). A constant value of Manning coefficient was applied to all computational grids except at the finest resolution (Region 6) were different Manning's roughness coefficients specified according to land use types and building density, as the effect of bottom friction on tsunami propagation in deep waters negligible. Tidal level was set to tide conditions at the time of tsunami occurrence in 2011 and simulation time was set to three hours. Initial water surface elevation was assumed to follow sea floor deformation and the fault parameters proposed by Tohoku University model (Imamura et al, 2016) were selected to reproduce the 2011 Great east Japan tsunami. Results of numerical simulation are shown in **Fig. 5**.

The accuracy of model is validated by comparing measured tsunami trace heights and modelled results (**Fig. 6**) using Aida's K and κ (Aida, 1978) as defined in equations (1) - (3) below.

$$\log K = \frac{1}{n}\sum_{i=1}^{n} \log K_i \qquad (1)$$

$$\log\kappa = \sqrt{\frac{1}{n}\sum_{i=1}^{n} (\log K_i)^2 - (\log K)^2} \qquad (2)$$

$$K_i = \frac{x_i}{y_i} \qquad (3)$$

Where, x_i and y_i are the measured and simulated tsunami trace heights (Mori et al., 2012) at point i. Consequently, K is regarded as a correction factor to adjust the modeled values to fit the actual tsunami averaged over several locations; κ is defined as a measure of the fluctuation or deviation in K_i. Values of Aida's K and κ are 1.04 and 1.32 respectively. The corrected tsunami simulation produced tsunami flow depths which are a close match to the measured tsunami trace heights and satisfy the guideline of the Japan Society of Civil Engineers (JSCE) ($0.95 < K < 1.05$ and $\kappa < 1.45$) (JSCE, 2016). Hence, tsunami flow depths and velocities in Ishinomaki City of higher accuracy were reproduced.

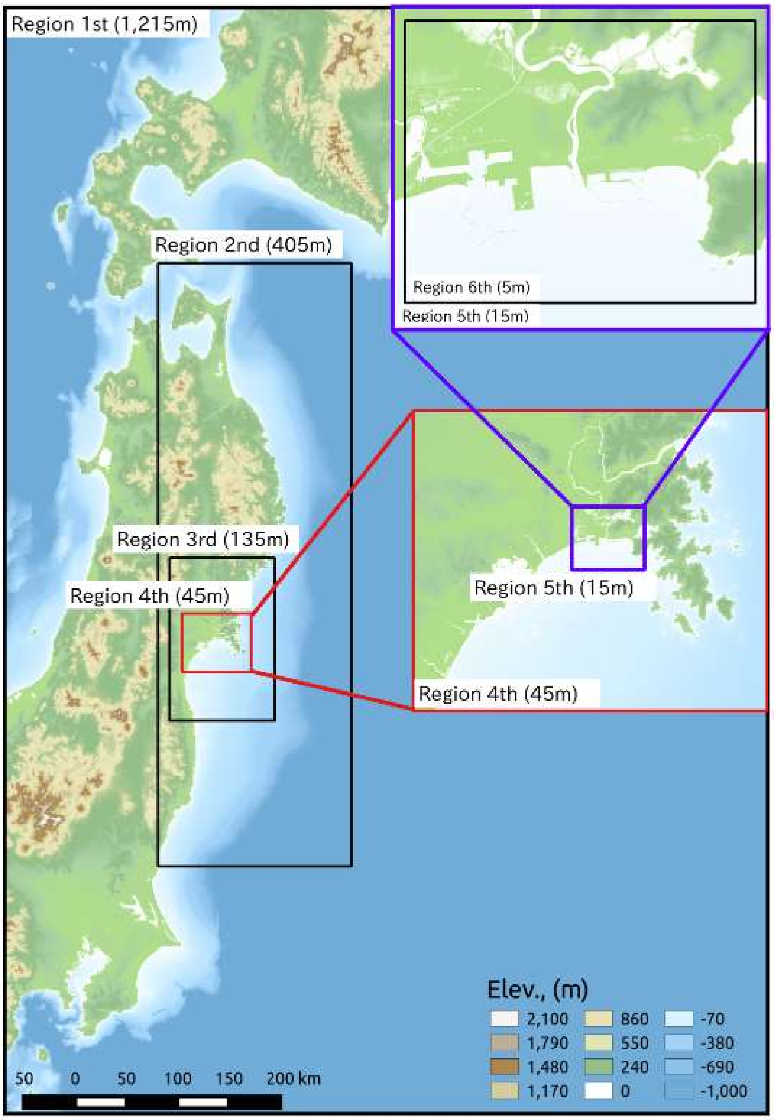

Fig.4 Computational regions in this study. Projection of bathymetry and topography data is the Japanese Geodetic Datum 2000 and the Tokyo Peil (T.P.) datum.

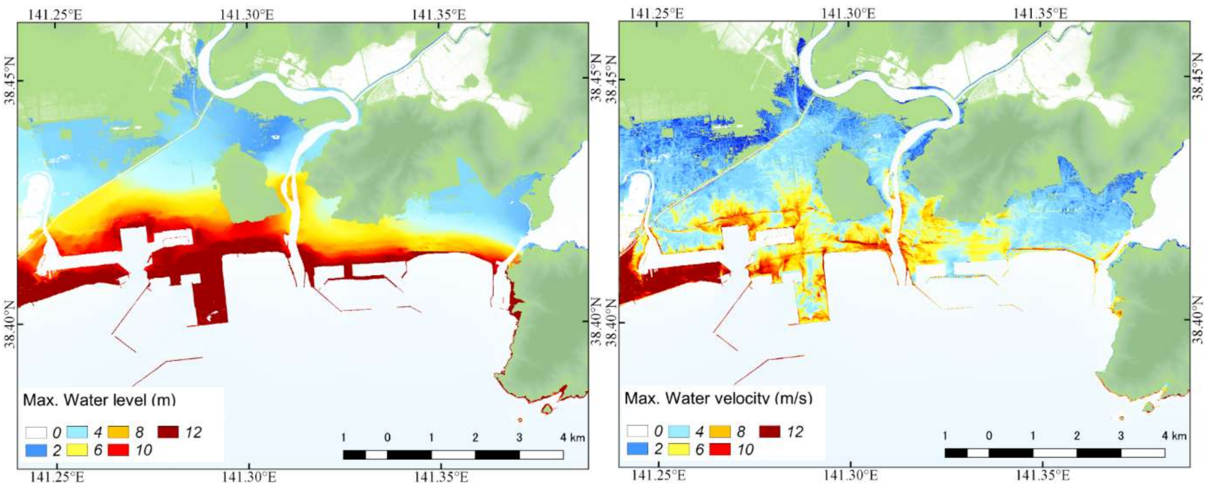

Fig. 5 Results of tsunami numerical simulation: (Left) Maximum flow depth and (Right) Maximum flow velocity.

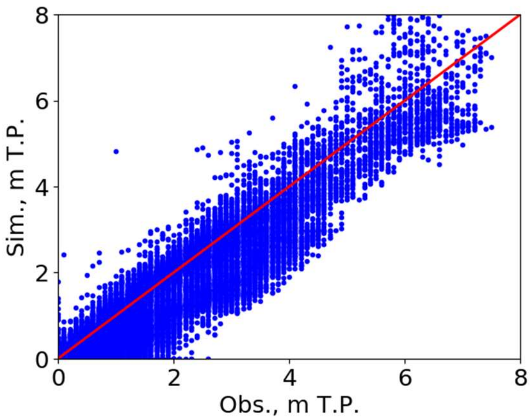

Fig. 6 Validation of the simulated tsunami inundation heights using the observed tsunami trace heights (Mori et al., 2012).

Results from the tsunami simulation were used to estimate tsunami-induced forces. Flow depth and velocity values were captured at each time step of the simulation and at each building location for more than 20,000 wooden buildings in Ishinomaki city. These values were then used to calculate hydrodynamic force (F_h) through drag formula (equation (4)), debris impact force (F_d) through impulse-momentum approach (equation (5)) as well as buoyancy force (B) (equation (6)) at each time step for each building (**Fig. 1**).

$$F_h = \frac{1}{2} C_D \rho u^2 D \tag{4}$$

$$F_d = m \frac{u}{\Delta t} \tag{5}$$

$$B = \rho g V \tag{6}$$

Where C_D denotes the drag coefficient (C_D = 1.5 as an average value from 1.25 to 2.00 depending on the width to depth ratio, FEMA, 2003), ρ the density of water (= 1, 000 kg/m^3), u the current velocity (m/s), D inundation depth (m), m (kg) the weight of debris, Δt the duration of impact (= 0.7 sec for wooden wall, FEMA, 2003), g the gravitational acceleration and V the submerged volume. This study follows the recommended weights of floating debris by the American's Federal Emergency Management Agency (FEMA, 2003) and Japan Society of Material Cycles and Waste Management (JSCWM, 2011), where the estimates were approximately 500 kg for a pine tree, 3,000 kg for a vehicle, and buildings - 15,000 kg, 30,000 kg and 60,000 kg for moderately damaged, majorly damaged and collapsed buildings respectively.

2.4 Resistant forces

In this study, the designed resistance of each building to withstand loads imposed on them is considered as its damage threshold. One aim is to determine if the modelled tsunami induced forces (i.e. hydrodynamic force, buoyancy force and debris impact force) for each building would exceed its damage threshold and therefore, result in damage to the building. As mentioned earlier, differences in the types of loads imposed and types of building resistance forces involved were considered when modelling sliding and overturning mechanism of a building. Both mechanisms were modelled separately. There are two types of resistant forces in a building i.e. vertical and lateral resistance. The vertical resistance of a building is its weight, and in this study, it was assumed to be 3,000 kN/m^2 for each building (Yokohama City, 2018). Vertical load-resistance analysis was used to determine overturning mechanisms.

For the first time, lateral resistance (R) from the bearing wall of a building will be considered when estimating building damage from tsunamis. The failure of lateral resistance of a building can imply that sliding mechanisms are involved in its collapse. The bearing wall of a building must be able to resist lateral loads imposed on them such as wind or seismic activity. The lateral resistance of each building to earthquake and wind forces was calculated in accordance with Article 46 Enforcement Ordinance of Building Standard Law (MLIT, 2018), and in which case, lateral resistance is the product of the lateral strength of the bearing wall and the required wall length of each building. The lateral strength of the bearing wall by Japanese housing design standard is 1.96 kN/m (MLIT, 2018).

Calculations for the required wall length would differ for both seismic and wind loads. Required wall length for seismic loads can be derived by taking the building's floor area and multiplying it by its design coefficient for seismic load (**Fig. 7**) (MLIT, 2018) as illustrated in Example 1. On the other hand, for wind loads, the required wall length can be calculated by multiplying the design coefficients with the vertical projection area (both the front and side of the building) (MLIT, 2018) as illustrated in Example 2. The vertical projection area is the area defined by the building width or length multiplied by the floor height above 1.35 m (**Fig. 8**). As information on building heights in Ishinomaki city was not available at the point of this study, an anonymous interview was conducted with a local housing construction company. The estimates provided for the heights of the first, second and third floors of an average wooden housing were 3.5 m, 2.7 m and 2.1 m respectively, which were then used as the average values for the purpose of this study. Wooden buildings in Ishinomaki city did not exceed three stories.

In this study, the lateral resistance of a building against tsunami impacts is considered as the sum of lateral resistance for floors below the modelled maximum flow depth. Estimation of lateral resistance for buildings should be taken with care as it was calculated for each floor. The total lateral resistance of a building against seismic or wind loads would be the sum of lateral resistance for every floor where maximum tsunami flow depth has reached. The highest estimated lateral resistance between seismic and wind loads was then chosen as the maximum effective resistance, hence the assumed lateral resistance design for each building. It should also be noted that the design lateral resistance may decrease due to age and ground shaking from previous earthquakes. A previous study done by the Japan Building Disaster Prevention Association (2012) reported 0.7 as the minimum reduction coefficient to account for these effects. Therefore, a range of bearing wall resistance reduction coefficients (0.7, 0.8, 0.9 and 1.0) was introduced when calculating the lateral resistance of the building.

Example 1

Calculation example of required wall length for seismic load

One story with 60 m^2 of floor area, the required wall length = 60 m^2 × 15 cm/m^2 = 900 cm = 9 m

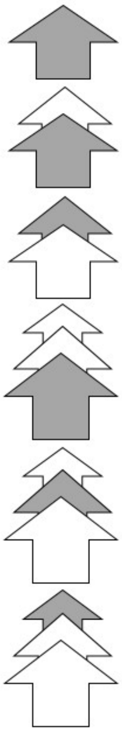

15 cm/m^2	One story building
33 cm/m^2	The first floor of two stories building
21 cm/m^2	The second floor of two stories
50 cm/m^2	The first floor of three stories building
39 cm/m^2	The second floor of three stories building
24cm/m^2	The third floor of three stories building

Fig. 7 Design coefficients for calculating corresponding necessary wall length against seismic load for 1-3 stories wooden houses (MLIT, 2018).

<u>Example 2</u>

Calculation example of required wall length for wind load

The first floor of two stories building,

Front: Required wall length = ①A (m^2) × 50 cm/m^2

Side: Required wall length = ②B (m^2) × 50 cm/ m^2

The second floor of two stories building

Front: Required wall length = ②A (m^2) × 50 cm/m^2

Side: Required wall length = ②B (m^2) × 50 cm/ m^2

The design wall length for wind load will be the summation of the maximum value at each floor.

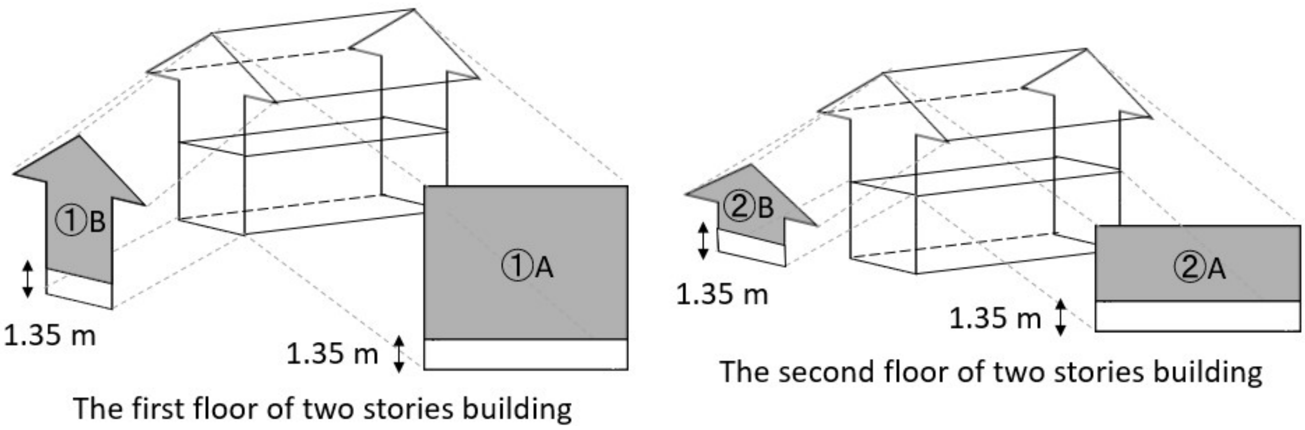

Fig. 8 Calculation example of corresponding necessary wall length against wind load.

2.5 Building damage replacement cost ratio

Although financial loss is not the central focus of this paper, it is a good opportunity to present a potential building damage replacement cost index for wooden buildings for future loss estimates. At present, tsunami building damage costs are based on data obtained from insurance claims after tsunami events. Loss estimates are, for the most part, based on analyses which are separate from the damage assessments and they do not account for building conditions and tsunami hydrodynamics.

The building damage levels proposed by MLIT (**Fig. 3**) formed the basis of developing the replacement cost index. Throughout this study, the focus has been on collapsed buildings (levels 5 and 6). This index however will be representative of both collapsed and non-collapsed buildings. Collapsed buildings can automatically be assigned as 100% loss as they are assumed to be irreparable. In general, construction costs of two-storey wooden houses in Japan comprise two components – architectural works which forms 70% of total costs and structural works which forms 30%. Costs of structural works can be further broken down into non-structural components (roofs (20%) and walls (10%)) and structural components (beams (20%), columns (15%) and footings (45%)) of the building. The averaged numbers of each component were calculated based on actual data of several houses (MN Housing and Building Laboratory, 2015, Cabinet Office of Japan, 2017, and Japan Wood-Products Information and Research Center, 2019).

3. Results and discussion

3.1 Accuracy of the proposed building damage assessment method

The results of the proposed building damage assessment model were compared to field observations to assess its performance (**Fig. 9**). Field observations are presented in the MLIT database and only buildings with damage levels 5 and 6 (collapse conditions) were used for comparison. **Table 1** shows an accuracy of modelled collapsed buildings and actual collapsed buildings from field observations when only sliding mechanism was considered, and **Table 2** when both sliding and overturning mechanisms were considered. Both tables have clearly illustrated that debris impact forces and resistance reduction coefficients do not seem to have significantly influenced the collapse of buildings in Ishinomaki. Damage analysis without debris weight input and building resistance reduction coefficient showed a better match. This can be attributed to the fact that Ishinomaki city was not heavily affected by floating debris for the reasons stated in **section 3.1.**

Tables 1 and **2** highlight sliding mechanism alone is a poor explanation of collapse. In other words, overturning is an important mechanism when analyzing building collapse. When using the proposed method, the modelled results show a near 100% accuracy, as shown in **Table 2** and illustrated in **Fig. 9**.

Table 1 Damage assessment accuracy (%): Washed away and destroyed buildings (damage levels 5 and 6) by considering only sliding as damage mechanism.

Debris weight	Resistance reduction coefficient			
	1	0.9	0.8	0.7
0 ton	65.24	66.54	68.02	69.84
0.5 tons	59.27	60.44	61.86	63.61
3 tons	61.43	62.92	64.55	66.39
15 tons	67.45	68.88	70.56	72.26
30 tons	72.44	72.21	71.13	69.43

60 tons	89.32	89.40	89.49	59.48

Table 2 Damage assessment accuracy (%): Washed away and destroyed buildings (damage levels 5 and 6) by considering both damage mechanisms.

Debris weight	Resistance reduction coefficient			
	1	0.9	0.8	0.7
0 ton	99.79	99.77	99.73	99.69
0.5 tons	96.46	96.44	96.40	96.35
3 tons	96.29	96.19	96.03	95.81
15 tons	91.97	91.25	90.17	88.96
30 tons	85.37	83.71	81.67	79.49
60 tons	93.73	93.77	93.83	72.26

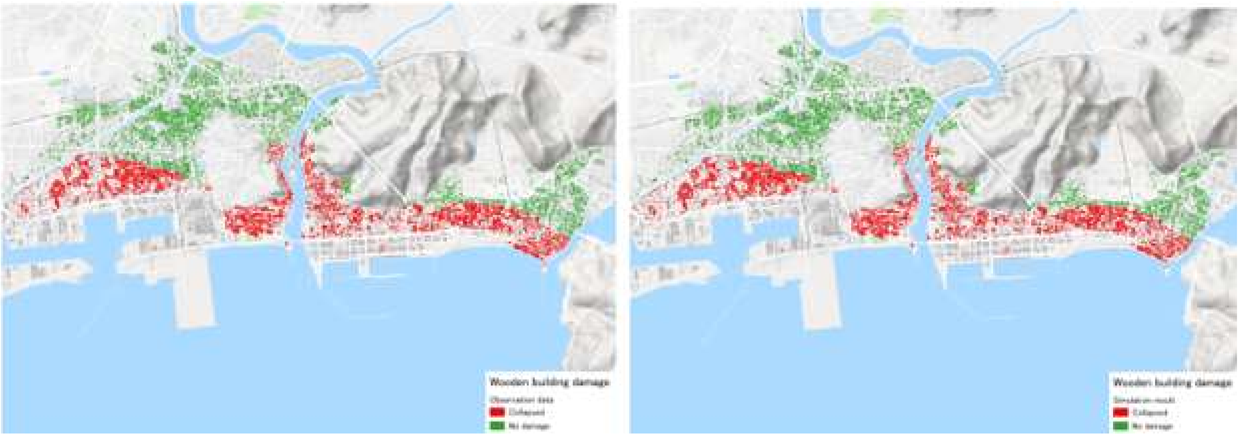

Fig. 9 Distributions of collapsed and non-collapsed buildings from field observation (left) and the proposed method (right)

3.2 Comparison of minimum load values for the collapse of wooden buildings against field observations and hydraulic experiments

The average lateral resistance of a building in Ishinomaki, derived from 19, 000 wooden houses in this study, is estimated to be about 42 kN, and the average hydrodynamic force is about 10 kN. These findings are evaluated and compared to other findings in tsunami literature to understand the dominant mechanism of building collapse. In a hydraulic experiment by Arikawa (2009), the flexural capacity of a wooden wall was tested. A wooden wall (2.5 m high and 2.7 wide) supported by a steel frame was placed in a water flume in a full-scale experiment. The wooden wall was found to be destroyed at a tsunami flow depth of 2.5 m. The flexural capacity of the wooden wall was 10 kN/m^2, which is equivalent to 67.5 kN. Matsutomi and Harada (2010) measured tsunami flow depth at the front and back of buildings during their field survey. Based on the survey and estimated Froude number, they found that for wooden houses, the necessary lateral force required to cause moderate damage is 5.4 – 9.9 kN/m and for major damage is 9.7 – 17.6 kN/m. Therefore, the minimal lateral load required for wooden houses to be washed away is approximately 9.7 – 17.6 kN/m or 88 -176 kN, assuming that the width of the house is 5 – 10 m. This information further supports the consideration of overturning as a critical explanation for collapse mechanism.

3.3 Tsunami characteristics at the time of collapse and influence of flow characteristics on damage

Critical flow depth (D_c) and critical flow velocity (V_c) values are flow depths and velocities at the time of building collapse or rather, when buildings were considered collapsed when using the proposed damage model. In this study, a further assessment was made to derive maximum flow values and compare them to the critical values modelled for each building. In general, the critical values are lower than maximum values for both flow depth and velocity (**Figs. 10 & 11**). The maximum flow depth (D_m) is about four times higher than the critical flow depth and maximum flow velocity (V_m) is about two times higher than the critical flow velocity (**Table 3**). The implication is straightforward – building damage would be highly underestimated when using maximum flow characteristics as explanatory variables. It underscores one of the weaknesses of using traditional tsunami damage assessment methodologies.

It is also observed that flow depth and flow velocity contribute differently to total building damage. Critical flow depth and velocity for collapsed (damage levels 5 and 6) and non-collapsed buildings are plotted in **Fig. 12** and it appears that wooden buildings would almost always get washed away when critical flow velocity exceeds 2 m/s, regardless of the value of critical flow depth. This value may serve as a simple indicative criterion to assess building damage potential. This criterion when used together with developed tsunami maps or numerical flow simulation allows for some initial building damage assessment and quick estimations.

The influence of flow depth and flow velocity on building damage may also vary across space. The relationship between critical and maximum flow depth values are represented as ratios and the distribution of these ratios are plotted in a map (**Fig. 13 (Left)**). Similarly, the distribution of the ratio between critical and maximum flow velocities are plotted in a map (**Fig. 13 (Right)**). Flow velocity appears to be a more significant parameter of damage (as ratios are close to 1.00) in areas nearer to the shoreline where flow velocity is very high and tsunami induced force is mostly hydrodynamic. On the other hand, flow depth has a greater influence on damage in areas nearer to the inundation limit where pressure from the tsunami is mostly hydrostatic.

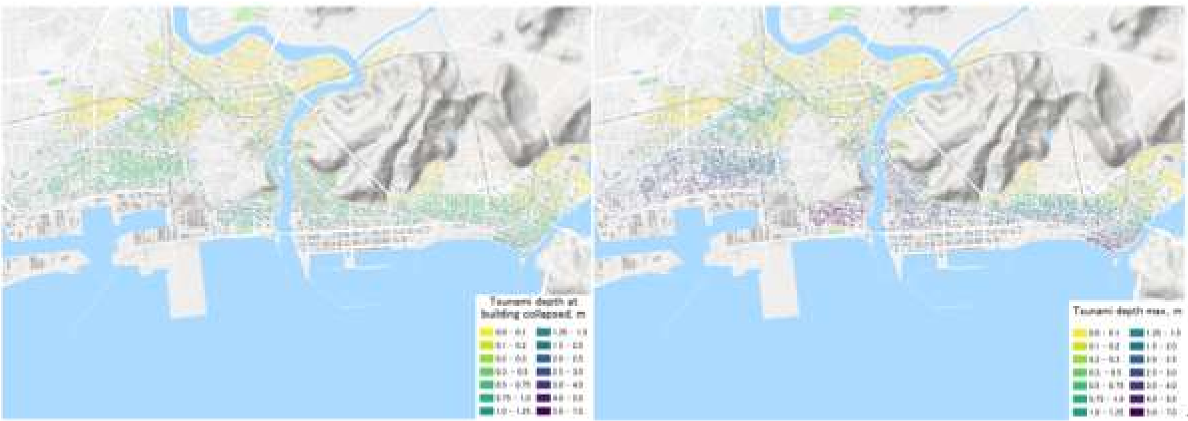

Fig. 10 Distribution of the simulated critical flow depth (left) and the simulated maximum flow depth (right)

Fig. 11 Distribution of the simulated critical flow velocity (left) and the simulated maximum flow velocity (right)

Table 3 Flow depth and velocity ratios (washed away and destroyed buildings: damages levels 5 and 6).

Damage conditions	D_m / D_c	V_m / V_c
Collapsed	4.03	2.34
Non-collapsed	1.56	1.16

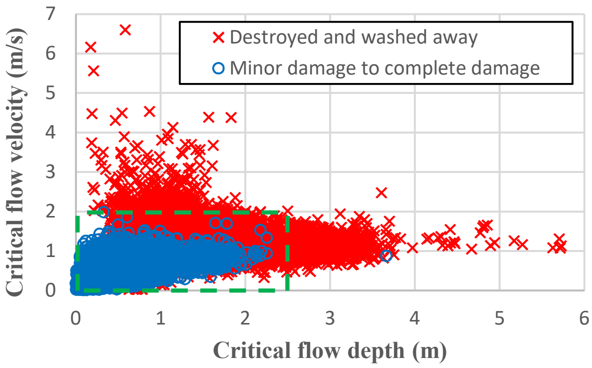

Fig.12 Plotting of the critical flow depth and critical flow velocity

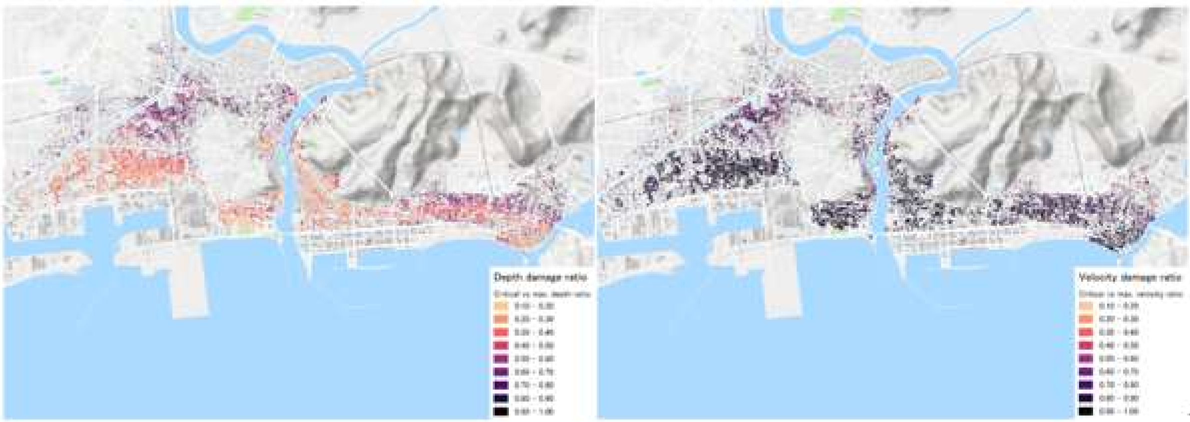

Fig. 13 Distributions of ratios between the critical and the maximum values of the simulated flow depth (left) and flow velocity (right). Higher ratios are found near inundation limit for the flow depth whereas near shoreline for the flow velocity.

3.4 Comparing results from fragility functions

Building collapse in Ishinomaki City was recently modelled by Hasegawa et al. (2018), where they developed fragility functions using the same building damage dataset (MLIT, 2012) and collapse criteria. The fragility functions were developed by applying logistic regression (where damage states follow a binomial distribution). The estimated damage probabilities are calculated as per equation (7). Values of the maximum likelihood estimations are presented in **Table 4**.

$$p = \frac{1}{1 + \exp(-a_0 - a_i x_i - \cdots)} \qquad (7)$$

Where p is a probability of collapse, a_n is a regression constant and x_n is an explanatory variable. In the damage assessment of this study, a building is classified as collapsed when the probability of collapse is higher than 50%.

Table 4 The maximum likelihood estimates (Hasegawa et al., 2018)

	Estimate	Stand. Error	Z value	Pr (>|z|)	p value
Constant term	-3.9250	0.0514	-76.4360	< 2e-16	*
RC building	-1.7970	0.0814	-22.0870	< 2e-16	*
Wooden building	1.4120	0.0440	32.1180	< 2e-16	*
Numbers of stories	-0.4242	0.0164	-25.8550	< 2e-16	*
Functions	0.2272	0.0277	8.2050	2.31E-16	*
Flow depth	1.0530	0.0060	174.1830	< 2e-16	*
Building area	-0.0003	0.0000	-7.1890	6.53E-13	*

p value: * < 0.001

Results from this study are compared to the fragility functions to determine how well building damage can be identified when using either the proposed method or the fragility functions. The building damage condition is reproduced using both methods and compared to actual observations as shown in **Fig. 14**. The proposed method is able to correctly reproduce collapsed and non-collapsed buildings with 99.79% accuracy, while the fragility functions are able to reproduce building damage conditions with 91.06% accuracy, as summarized in **Table 5**. It can be observed the model based on fragility functions does not perform as well when assessing building damage in the zone separating collapsed and non-collapsed buildings.

It should be noted that building damage assessment with such accuracy can only be replicated because of the strict construction design standards in Japan. How well the proposed method will perform in a context outside of Japan will be largely dependent on local practices in the design and construction of the buildings, the presence debris material and the age of the building (resistance reduction coefficients). Additionally, flow-building interactions which yield lower damage states are not accounted for, so the model may not perform as well for flow conditions which are less severe than the 2011 Great East Japan tsunami.

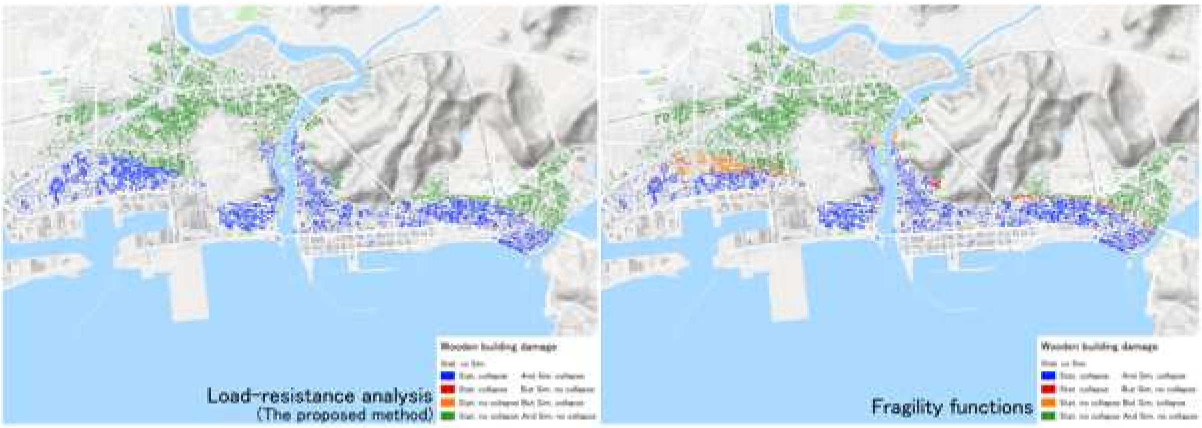

Fig. 14 Reproduction of building damage condition (collapse or non-collapse): Comparison between the proposed method and field observation (left) and Fragility functions and field observation (right). Blue: Correct reproduction of collapsed buildings, Green: Correct reproduction of non-collapsed buildings, Red: Failure to reproduce collapsed buildings and Orange: Failure to reproduce non-collapsed buildings.

Table 5 Building damage assessment accuracy of this proposed method and previously developed fragility functions compared to field observations. This table shows numbers of buildings for each condition and their accuracy percentages.

		Analytical method (this study)	
		Collapsed	Non-collapsed
Field observation	Collapsed	8,518 (45.22%)	33 (0.18%)
	Non-collapsed	7 (0.04%)	10,277 (54.56%)

		Fragility functions	
		Collapsed	Non-collapsed
Field observation	Collapsed	7,362 (39.09%)	1,189 (6.31%)
	Non-collapsed	519 (2.76%)	9,765 (51.85%)

3.5 Financial loss metrics

Damage ratio of each structural and non-structural component at each damage level was interpreted based on MLIT's building damage definition (MLIT, 2012). On account of approximations of the construction cost as presented in section 2.5, each building damage level defined by structural damage condition can be converted into replacement cost ratio as follows (**Table 6** and **Table 7**).

Table 6 MLIT's damage level classification, description and condition (MLIT, 2012) and the damage ratio for structural works and architectural works

Damage level	Classification	Description	Condition	Structural works	Architectural works
1	Minor damage	There is no significant structural or non-structural damage, possibly only minor flooding	Possible to be use immediately after minor floor and wall clean up	0%	25%
2	Moderate damage	Slight damages to non-structural components	Possible to be use after moderate reparation	10% to roof and wall	50%
3	Major damage	Heavy damages to some walls but no damages in columns	Possible to be use after major reparation	25% to roof and wall	75%
4	Complete damage	Heavy damages to several walls and some columns	Possible to be use after a complete reparation and retrofitting	50% to roof and wall 25% to beam and column	100%
5	Destroyed or collapsed	Destructive damage to walls (more than half of wall density) and several columns (bend or destroyed)	Loss of functionality (system collapse). Non-repairable or great cost for retrofitting	75% to roof and wall 50% to beam and column	100%
6	Washed away	Washed away, only foundation remained, total overturned	Non-repairable, requires total reconstruction	100% to all components	100%

Table 7 Summary of 1) ratio of the cost of structural works, 2) damage ratio of each structural and non-structural component at each damage level and 3) replacement cost ratio

Damage level	Roof	Beam	Column	Wall	Footing	Replacement cost ratio	Final replacement cost ratio
	0.1	0.2	0.15	0.1	0.45		
1	0	0	0	0	0	0.18	0.18
2	0.1	0	0	0.1	0	0.36	0.36
3	0.25	0	0	0.25	0	0.54	0.54
4	0.5	0.25	0.25	0.5	0	0.76	0.76
5	0.75	0.5	0.5	0.75	1	0.78	1.00
6	1	1	1	1	1	1.00	1.00

Damage level 1: Minor damage (Replacement cost ratio = 18%)
Because of its damage description as “no significant structural or non-structural damage, possibly only minor flooding”. A 25% architectural works is applied as the condition “Possible to be use immediately after minor floor and wall clean up”.
Replacement cost ratio $= 0.3\times[(0\times0.1)+(0\times0.2)+(0\times0.15)+(0\times0.1)+(0\times0.45)] + 0.7\times[0.25] = 0.18$

Damage level 2: Moderate damage (Replacement cost ratio = 36%)
A damage ratio of 10% is assigned to roof and wall according to the damage description “Slight damages to non-structural components”. A 50% architectural works is applied as the condition “Possible to be use after moderate reparation”.
Replacement cost ratio $= 0.3\times[(0.1\times0.1)+(0\times0.2)+(0\times0.15)+(0.1\times0.1)+(0\times0.45)] + 0.7\times[0.50] = 0.36$

Damage level 3: Major damage (Replacement cost ratio = 54%)
A damage ratio of 25% is assigned to roof and wall according to the damage description “Heavy damages to some walls but no damages in columns”. A 75% architectural works is applied as the condition “Possible to be use after major reparation”.
Replacement cost ratio $= 0.3\times[(0.25\times0.1)+(0\times0.2)+(0\times0.15)+(0.25\times0.1)+(0\times0.45)] + 0.7\times[0.75] = 0.5$

Damage level 4: Complete damage (Replacement cost ratio = 76%)
A damage ratio of 50% is assigned to roof and wall and 25% to beam and column according to the damage description “Heavy damages to several walls and some columns”. A 100% architectural works is applied as the condition “Possible to be use after a complete reparation and retrofitting”.
Replacement cost ratio

$$= 0.3\times[(0.5\times0.1)+(0.25\times0.2)+(0.25\times0.15)+(0.5\times0.1)+(0\times0.45)] + 0.7\times[1] = 0.76$$

Damage level 5: Collapsed (Replacement cost ratio = 100%)
A damage ratio of 75% is assigned to roof and wall and 50% to beam and column according to the damage description “Destructive damage to walls (more than half of wall density) and several columns (bend or destroyed). However, because a damage ratio of 100% is assigned to footing because of the damage condition “Non-repairable or great cost for retrofitting”, the final replacement cost ratio is set to 100%.
Replacement cost ratio

$$= 0.3\times[(0.75\times0.1)+(0.5\times0.2)+(0.5\times0.15)+(0.75\times0.1)+(1\times0.45)] + 0.7\times[1] = 0.78 \rightarrow 1.00$$

Damage level 6: Washed away (Replacement cost ratio = 100%)
A damage ratio of 100% is assigned to all structural components according to the damage description “Washed away, only foundation remained, total overturned” and damage condition “Non-repairable, requires total reconstruction”.

4. Conclusions

This study presented a novel quantitative tsunami damage prediction approach, load-resistance analysis. While previous empirical and experimental studies have vastly improved our understanding of building response to tsunami impacts and extensively quantified building damage characteristics, implementation of the resulting damage estimates for future tsunami scenarios is challenging; in particular, when spatial differences such as construction standards and coastal morphology are significant. Load-resistance analysis utilizes building design standards to estimate the resistance force of each building, hence analytically estimate the potential for building damage (collapse) in a localized context. One of the advantages of load-resistance analysis is it can be extended to other areas where existing empirical data is sparse, and modified to assess building collapse (sliding or overturning mechanism). This approach is complementary to published statistical tsunami damage fragility functions as demonstrated in the case study of Ishinomaki City.

To date, building damage characteristics have been treated separately from financial losses which are often of interest to policy makers and planners. This study is a first attempt to propose both building damage estimations and financial losses. Using the established classification of building damage by MLIT, building construction costs were evaluated and pegged to each damage level as replacement cost ratios. The proposed replacement cost index provide an approximate estimate of potential financial losses in areas where pre-existing disaster-related insurance claim settlements are lacking.

4.1 Main findings

Additional key findings emerging from this study are summarized below:

- Analytical estimation of the potential for building collapse was calculated using building design standards and accounting for resistance reduction coefficients, as well as tsunami hydrodynamic force considering different debris weights. The most general case (resistance reduction coefficient of 1.0 and 0 ton debris weight) yields the highest accuracy in estimating building collapse in Ishinomaki city.
- Sliding alone is an insufficient explanation for building collapse. It is also important to consider overturning mechanism.
- This study has confirmed that the use of maximum values for flow depth and velocity might underestimate damage. Damage is likely to occur before flow depth and velocity reach maximum values. The present results suggest a flow velocity of 2 m/s or more would trigger collapse for a typical Japanese 2 story residential wood building
- The ratio between critical flow velocity and maximum flow velocity might be a useful alternative damage intensity measure but needs further investigation – particularly in the light of intermediate damage levels.
- The proposed load-resistance analysis shows higher accuracy in assessing building collapse compared to previously developed fragility functions in the same study area.
- Replacement cost ratio for each level of MLIT damage classification are approximately 18%, 36%, 54%, 76%, 100% and 100% for damage levels 1, 2, 3, 4, 5 and 6 respectively.

4.2 Future applications and limitations

The newly proposed load-resistance analytical method can be applied to other coastal regions of Japan and globally, only where building design standards and related information are known and enforced. However, such detailed analyses require higher computational cost and data storage. The proposed method may only work in countries where building design codes are strictly followed as in the case of Japan and for events generating heavy levels of damage. Additionally, the reliability of building damage predictions using this method is dependent on the accuracy of the numerical model. This depends on the availability and quality of information regarding the hazard, the dominant damage mode assumed in the analysis and/or reference dataset, the assumed debris weight coefficient and the resistance reduction coefficient employed. In absence of such information, building damage estimates are subjected to significant uncertainty. Therefore, the application of this method is not to produce absolute figures for damage estimates, but to be a useful guideline for planning purposes and an alternative study for comparison.

Acknowledgments

This research was funded and supported by JSPS Grant-in-Aid for Young Scientists (B) "Applying developed fragility functions for the Global Tsunami Model (GTM)" (Grant No. 16K16371), JSPS-NRCT Bilateral Research grant, the Core Research Cluster of Disaster Science in Tohoku University (Designated National University), Tokio Marine & Nichido Fire Insurance Co., Ltd., Willis Research Network (WRN) and the Radchadapisek Sompoch Endowment Fund (2019), Chulalongkorn University (762003-CC).

References

1) Aida, I.: Reliability of a tsunami source model derived from fault parameters, J. Phys. Earth, 26, 57–73, 1978.
2) Arikawa, T.: Structural behavior under impulsive tsunami loading, Journal of Disaster Research, 4 (6), 377-381, 2009.
3) Attary, N., van de Lindt, J. W., Unnikrishnan, V. U., Barbosa, A. R., and Cox, D. T.: Methodology for development of physics-based tsunami fragilities, Journal of Structural Engineering, 143 (5), 04016223, 2017.
4) Cabinet Office of Japan: Chapter 2: Damage from water-related disasters, 72 p, 2017 Available at: http://www.bousai.go.jp/taisaku/pdf/h3003shishin_3.pdf (In Japanese) Accessed date: 28/9/2018
5) Charvet, I., Macabuag, J., and Rossetto, T.: Estimating tsunami induced building damage through fragility functions: Critical review and research needs, Front. Built Environ., 3, 1–22, 2017. https://doi.org/10.3389/fbuil.2017.00036
6) Charvet, I., Suppasri, A., Kimura, H., Sugawara, D., and Imamura, F.: Fragility estimations for Kesennuma City following the 2011 Great East Japan Tsunami based on maximum flow depths, velocities and debris impact, with evaluation of the ordinal model's predictive accuracy, Natural hazards, 79(3), 2073-2099, 2015.
7) Dall'Osso, F., Dominey-Howes, D., Tarbotton, C., Summerhayes, S., and Withycombe, G.: Revision and improvement of the PTVA-3 model for assessing tsunami building vulnerability using "international expert judgment": introducing the PTVA-4 model, Natural Hazards, 83 (2), 1229-1256, 2016.
8) Dias, W.P.S., Yapa, H.D., and Peiris, L.M.N.: Tsunami vulnerability functions from field surveys and Monte Carlo simulation, Civil Engineering and Environmental Systems, 26 (2), 181-194, 2009.
9) Federal Emergency Management Agency (FEMA): Tsunami methodology technical manual., Washington,DC, 2013.
10) Federal Emergency Management Agency (FEMA): Coastal Construction Manual (3 Vols.), 3rd edn. (FEMA 55) (Jessup, MD, 2003), 2013.
11) Hasegawa, N., Suppasri, A., Makinoshima, F., and Imamura, F.: A proposal of formula for damage prediction of each building using actual damage data from the 2011 Great East Japan tsunami, in Proceedings of the Annual Conference of JSCE Tohoku branch, II-97, 2018 (in Japanese).
12) Imamura, F.: Review of tsunami simulation with a finite difference method, in H. Yeh, P. Liu, and C. E. Synolakis (Eds.), "Long-Wave Runup Models," pp. 25-42, Singapore: World Scientific Publishing Co., 1996.
13) Imamura, F., Koshimura, S., Mabuchi, Y., Oie, T., and Okada, K.: Tsunami simulation of the 2011 Great East Japan Tsunami using Tohoku University model (Version 1.1), 2011 Available at http://www.tsunami.civil.tohoku.ac.jp (In Japanese) (Accessed date: 7 November 2011)
14) Japan Building Disaster Prevention Association: Seismic evaluation (General evaluation method) Pro Ver. 3.01, 18 pages, 2012 (In Japanese)
15) Japan Society of Civil Engineers (JSCE): Tsunami assessment method for nuclear power plants in Japan, available at: http://www.jsce.or.jp/committee/ceofnp/Tsunami/eng/JSCE_Tsunami_060519.pdf

(Accessed date: 6 August 2016)

16) Japan Society of Material Cycles and Waste Management, Disaster Waste Countermeasure and Reconstruction Task Team: Disaster waste classification and treatment strategy manual Version 2, the last update on 15 June 2011, available at http://eprc.kyoto-u.ac.jp/saigai/report/2011/04/001407.html (Accessed date: 14 February 2018) (In Japanese)

17) Japan Wood-Products Information and Research Center: O&A on utilization of wooden materials, 2019 Available at: http://www.jawic.or.jp/qanda/index.php?no=19 (In Japanese) Accessed date: 28/9/2018

18) Kelman, I., and Spence, R.: An overview of flood actions on buildings. Engineering Geology, *73*(3-4), 297-309, 2004.

19) Koshimura, S., Oie, T., Yanagisawa, H., and Imamura, F.: Developing Fragility Functions for Tsunami Damage Estimation using Numerical Model and Post-Tsunami Data from Banda Aceh, Indonesia, Coast. Eng. J., 51, 243–273, 2009.

20) Latcharote, P., Suppasri, A., Yamashita, A., Adriano, B., Koshimura, S., Kai, Y., and Imamura, F.: Possible Failure Mechanism of Buildings Overturned during the 2011 Great East Japan Tsunami in the Town of Onagawa, Frontiers in Built Environment, Earthquake Engineering, Mega Quakes: Cascading Earthquake Hazards and Compounding Risks, 3 (16), 1-18, 2017.

21) Leelawat, N., Suppasri, A., Charvet, I., and Imamura, F.: Building damage from the 2011 Great East Japan tsunami: Quantitative assessment of influential factors - A new perspective on building damage analysis, Natural Hazards, 73 (2), 449-471, 2014.

22) Macabuag, J., Rossetto, T., Ioannou, I. and Eames, I.: Investigation of the effect of debris-induced damage for constructing tsunami fragility curves for building, Geosciences 2018, 8(4), 117, 2018.

23) Macabuag, J., Rossetto, T., Ioannou, I., Suppasri, A., Sugawara, D., Adriano, B., Imamura, F. and Koshimura, S.: A proposed methodology for deriving tsunami fragility functions for buildings using optimum intensity measures, Natural Hazards, 84 (2), 1257-1285, 2016.

24) Macabuag J., Rossetto T., and Lloyd T.: Sensitivity analysis of a framed structure under several tsunami design-guidance loading regimes. 2nd European Conference on Earthquake Engineering and Seismology, Istanbul, Turkey, 2014.

25) Matsutomi, H. and Harada, K.: Tsunami-trace distribution around building and its practical use, in: Proceedings of the 3rd International tsunami field symposium, Sendai, Japan, 10–11 April 2010, session 3–2, 2010.

26) MN Housing and Building Laboratory: Wooden house cost simulation, 2015 Available at: http://mnsekkei-cost.blogspot.com/ (In Japanese) Accessed date: 28/9/2018

27) Mori, N., Takahashi, T., and 2011 Tohoku Earthquake Tsunami Joint Survey Group: Nationwide Post Event Survey and Analysis of the 2011 Tohoku Earthquake Tsunami, Coastal Engineering Journal, 54, 1250001, 2012.

28) Ministry of Land, Infrastructure, Transportation and Tourism (MLIT): Reconstruction Support Survey Archive: http://fukkou.csis.u-tokyo.ac.jp/ (Accessed date: 4 July 2012) (In Japanese)

29) Ministry of Land, Infrastructure, Transportation and Tour-ism (MLIT), Article 46 Enforcement Ordinance of Building Standard Law, 2018 Available at: http://elaws.e-gov.go.jp/search/elawsSearch/elaws_search/lsg0500/detail?lawId=325CO0000000338#390 (Accessed date: 15 January 2018) (In Japanese)

30) Nadal, N. C., Zapata, R. E., Pagán, I., López, R., and Agudelo, J.: Building damage due to riverine and coastal floods. Journal of Water Resources Planning and Management, 136(3), 327-336, 2009.

31) Nanayakkara, K. and Dias, W.: Fragility curves for structures under tsunami loading, Natural Hazards, 80 (1), 471-486, 2016.

32) Omira, R., Baptista, M. A., Miranda, J. M., Toto, E., Catita, C., and Catalão, J.: Tsunami vulnerability assessment of Casablanca Morocco using numerical modelling and GIS tools. Natural Hazards, 54, 75–95, 2010.

33) Peiris, N.: Vulnerability functions for tsunami loss estimation, The 1st European Conference on Earthquake Engineering and Seismology, Geneva, Switzerland, 3-8 September 2006, Paper no. 1121, 10 pages.

34) Reese, S., Cousins, W. J., Power, W. L., Palmer, N. G., Tejakusuma, I. G., and Nugrahadi, S.: Tsunami vulnerability of buildings and people in South Java? Field observations after the July 2006 Java tsunami. Natural Hazards and Earth Systems Sciences, 7, 573–589, 2007.

35) Shoji, G. and Nakamura, T.: Damage assessment of road bridges subjected to the 2011 Tohoku Pacific earthquake tsunami, Journal of Disaster Research, 12, 79–89, 2017.
36) Song, J., De Risi, R., and Goda, K.: Influence of flow velocity on tsunami loss estimation, Geosciences 2017, 7(4), 114, 2017.
37) Suppasri, A., Fukui, K., Yamashita, K., Leelawat, N., Ohira, H., and Imamura, F.: Developing fragility functions for aquaculture rafts and eelgrass in the case of the 2011 Great East Japan tsunami, Nat. Hazards Earth Syst. Sci., 18, 145-155,2018.
38) Suppasri, A., Latcharote, P., Bricker, J. D., Leelawat, N., Hayashi, A., Yamashita, K., Makinoshima, F., Roeber, V., and Imamura, F.: Improvement of tsunami countermeasures based on lessons from the 2011 great east japan earthquake and tsunami-Situation after five years-, Coastal Engineering Journal, 58, 1640011, 2016.
39) Suppasri, A., Charvet, I., Imai, K., and Imamura, F.: Fragility curves based on data from the 2011 Great East Japan tsunami in Ishinomaki city with discussion of parameters influencing building damage, Earthquake Spectra, Vol. 31, No. 2, 841-868, 2015.
40) Suppasri, A., Muhari, A., Futami, T., Imamura, F., and Shuto, N.: Loss functions of small marine vessels based on surveyed data and numerical simulation of the 2011 Great East Japan tsunami, J. Waterway, Port, Coastal, Ocean Eng., 140, 04014018, 2014.
41) Suppasri, A., Koshimura, S., and Imamura, F.: Developing tsunami fragility curves based on the satellite remote sensing and the numerical modeling of the 2004 Indian Ocean tsunami in Thailand, Natural Hazards and Earth System Sciences, 11, 173–189, 2011.
42) Valencia, N., Gardi, A., Gauraz, A., Leone, F., and Guillande, R.: New tsunami damage functions developed in the framework of SCHEMA project: Application to European-Mediterranean coasts. Natural Hazards and Earth Systems Sciences, 11, 2835–2846, 2011.
43) Triantafyllou, I., Novikova, T., Charalampakis, M., Fokaefs, A., and Papadopoulos, G. A.: Quantitative Tsunami Risk Assessment in Terms of Building Replacement Cost Based on Tsunami Modelling and GIS Methods: The Case of Crete Isl., Hellenic Arc, Pure and Applied Geophysics, 2018 (Published online)
44) Yeh, H., Barbosa, A. R., Ko, H., and Cawley, J. G.: Tsunami loadings on structures: Review and analysis. Coastal Engineering Proceedings, 1(34), 4, 2014.
45) Yokohama City, Housing and Architecture Bureau: Standard weight table of wooden house and standard weight table calculation basis of wooden house, 2018 Available at http://www.city.yokohama.lg.jp/kenchiku/shidou/shidou/toriatukai/gakeue/siryou3.pdf (Accessed date: 21 February 2018) (In Japanese)